Close-up view of the modifications of fluid membranes due to phospholipase A_2

2005 J. Phys.: Condens. Matter 17 S4015

(http://iopscience.iop.org/0953-8984/17/47/025)

INSTITUTE OF PHYSICS PUBLISHING JOURNAL OF PHYSICS: CONDENSED MATTER

J. Phys.: Condens. Matter **17** (2005) S4015–S4024 doi:10.1088/0953-8984/17/47/025

Close-up view of the modifications of fluid membranes due to phospholipase A_2

Ask F Jakobsen[1,2], **Ole G Mouritsen**[1] **and Matthias Weiss**[2,3]

[1] MEMPHYS-Center for Biomembrane Physics, Physics Department, University of Southern Denmark, Campusvej 55, DK-5230 Odense M, Denmark
[2] Cellular Biophysics Group (BIOMS), German Cancer Research Center, Im Neuenheimer Feld 580, D-69121 Heidelberg, Germany

E-mail: m.weiss@dkfz.de

Received 10 August 2005
Published 4 November 2005
Online at stacks.iop.org/JPhysCM/17/S4015

Abstract

Phospholipases are a class of molecular machines that are involved in the active remodelling processes of biological membranes. These lipases are interfacially activated enzymes and in the specific case of phospholipase A_2 (PLA_2) the enzyme catalyses the hydrolysis of di-acyl phospholipids into products of lysolipids and fatty acids, that dramatically change the physical properties of lipid membrane substrates. Using dissipative particle dynamics simulations on a simple coarse-grained bead–spring model of a fluid lipid bilayer in water, the mechanical and diffusive properties of the bilayer in the pure state and after the action of PLA_2 have been calculated. It is found that, in response to hydrolysis, the lipid membrane becomes mechanically softened and the various in-plane and trans-bilayer diffusional modes become enhanced. The results compare favourably with available experimental data.

1. Introduction

Lipids constitute the basis for all living cells since they are the basic ingredient for making an engulfing plasma membrane which defines the cell in the first place. In eukaryotes also cellular organelles like endosomes, the endoplasmic reticulum (ER) and the Golgi apparatus are defined via distinct biomembranes (see [1] for a detailed introduction). Moreover, lipid-derived structures like vesicular carriers and tubules play a major role in cellular protein traffic, e.g. in the secretory pathway [2]. Due to the complex tasks that membranes are involved in, it is evident that they have to be very dynamic in composition and morphology. Peripheral membrane proteins play here a key role as regulators of membrane shape, composition, and elastic parameters. For example, the concerted action of coat proteins and small GTPases that

[3] Author to whom any correspondence should be addressed.

recruit the coat are crucial for making transport vesicles in the ER and the Golgi apparatus, respectively (see [3] for a review of the various types of vesicles).

Besides these drastic topological changes, peripheral membrane proteins are also responsible for more subtle events that facilitate the constant dynamical remodelling of membranes in living cells. Phospholipases, for example, play an active role in lipid metabolism and therefore are actively changing the composition and thus the response behaviour of native biomembranes. One particularly well investigated enzyme of this class is the water-soluble phospholipase A_2(PLA_2), that catalyses the hydrolysis of the *sn*-2 acyl ester linkage of *sn*-glycero-3-phospholipids [4]. The cleavage products are fatty acids and 1-acyl-lysolipids, which can locally alter the membrane's properties, e.g. the local bending stiffness and diffusion coefficients. In fact, PLA_2 is a family of interfacially activated enzymes that occur in different contexts [5]. $iPLA_2$, for example, occurs in macrophages and was suggested to play a role in endocytosis, while $sPLA_2$ is found in snake and bee venoms, pancreatic secretions and inflammatory fluids. $cPLA_2$ on the other hand is a widely expressed cytosolic protein that is, for example, important for the secretion of lung surfactant. Interestingly, $cPLA_2$ is activated by the tumour necrosis factor-α, a trigger of cell death and an important mediator of several autoimmune diseases and chronic inflammations [6]. Also, elevated levels of $sPLA_2$ and $cPLA_2$ have been reported in several tumour tissues, which makes PLA_2 a promising target for drug cancer treatment [7] and as a trigger to unload the drug of liposomal carriers specifically at diseased tissue [8]. Seeing PLA_2 in the context of cell death, it is also noteworthy that high levels of PLA_2 are found in tear drops, where it acts as a natural antibiotic and prevents infection of the eyes. It is worthwhile to mention that except $iPLA_2$ all PLA_2 isoforms need elevated Ca^{2+} levels for proper function.

Despite their potentially destructive action, most isoforms of PLA_2 only locally alter the properties of the membrane without affecting its integrity due to extensive regulation by cofactors. Also, the hydrolysis kinetics of PLA_2 depends on the morphology and physico-chemical state of the membrane substrate [9]. It has been reported that the rate of hydrolysis is initially fairly low and can suddenly increase by two to three orders of magnitude (lag–burst behaviour) [10–12]. This increase in activity is most likely related to the state of the substrate, i.e. the accumulation of cleavage products may alter the local morphology, which can stimulate further hydrolysis. Using atomic force microscopy, it has also been shown that PLA_2 can exhibit a short-ranged directed movement while digesting one leaflet of a membrane [13–15]. This phenomenon appears to be linked to the intrinsic structure of the membrane as the directed motion so far has only been observed in the gel or ripple phase of a bilayer.

Whereas there exists a large experimental literature on PLA_2 action on lipid bilayers, only very few theoretical and computational studies have been reported. The reason for this situation is the complexity of the problem, which is inherently a non-equilibrium problem, as well as a lack of appropriate models and efficient computational schemes. Some studies using lattice-gas models and Monte Carlo simulation have considered PLA_2 activation near lipid membrane phase transitions in equilibrium [11, 9] and away from equilibrium [17, 16]. Effective field theoretical models have also been used to model the activation in the neighbourhood of the solid–fluid phase transition [18–20]. In none of these studies have the self-assembly properties of the lipid system been taken into account and none of the theoretical models operate on a level of description where the mechanical and diffusional properties of the system can faithfully be extracted.

In this paper, we investigate how the mechanical and diffusional properties of a lipid bilayer membrane in its fluid phase become altered by the action of PLA_2. We do not model the action of the enzyme directly but only indirectly via the effects which arise upon introduction of various concentrations of hydrolysis products into the bilayer. The lipids in water are modelled

by simple coarse-grained molecules composed of hydrophilic and hydrophobic beads. In order to simulate the structural and dynamical properties of the model we have used dissipative particle dynamics (DPD), which is essentially a coarse-grained molecular dynamics approach. The paper is structured as follows: after the introduction, we introduce the concept of DPD in section 2 and define the simulation set-up. In section 3 we report on the mechanical properties of an unperturbed fluid membrane in order to provide a comparison with the results presented in section 4, where the mechanical and diffusional properties of membranes suffering from different concentrations of hydrolysis products are reported. Finally, we discuss our findings in section 5. Throughout the paper the simulation results are compared with experimental data when available.

2. Dissipative particle dynamics

Dissipative particle dynamics (DPD) is a coarse-grained molecular dynamics simulation method that aims at a mesoscopic rather than an atomistic description of many-particle systems. The individual molecules are modelled by beads that represent a number of atomic groups. Lipid molecules consist of several beads connected by springs whereas water is represented by a single bead. The basic ingredients are (i) soft-repulsive non-bonded interactions to achieve a mesoscopic simulation technique, and (ii) a special thermostat, implemented by means of pairwise dissipative and stochastic forces that conserve momentum locally in contrast to standard Langevin dynamics [21, 22]. Consequently, the method is, in principle, able to capture hydrodynamic behaviour which may be essential for observing the self-assembly of complex meso-phases of soft matter in coarse-grained simulations.

The dissipative forces between beads i and j that enter the DPD thermostat are given by

$$\mathbf{F}_{ij}^{D} = \begin{cases} -\gamma_{ij}(1 - r_{ij}/r_0)^2\,(\hat{\mathbf{r}}_{ij} \cdot \mathbf{v}_{ij})\hat{\mathbf{r}}_{ij}, & r < r_0, \\ 0, & r \geqslant r_0, \end{cases} \tag{1}$$

where γ_{ij} is the dissipation strength for two beads i, j which are located at positions $\mathbf{r}_i$ and $\mathbf{r}_j$ and have velocities $\mathbf{v}_i$ and $\mathbf{v}_j$, respectively. The position and velocity difference vectors are obtained as $\mathbf{r}_{ij} = \mathbf{r}_i - \mathbf{r}_j$ and $\mathbf{v}_{ij} = \mathbf{v}_i - \mathbf{v}_j$, while $\hat{\mathbf{r}}_{ij} = \mathbf{r}_{ij}/|\mathbf{r}_{ij}|$ denotes the unit vector. The random force is given by

$$\mathbf{F}_{ij}^{R} = \begin{cases} \sigma_{ij}(1 - r_{ij}/r_0)\zeta_{ij}\hat{\mathbf{r}}_{ij}, & r < r_0, \\ 0, & r \geqslant r_0, \end{cases} \tag{2}$$

where σ_{ij} is the random noise strength for beads i and j, and ζ_{ij} is a random variable with zero mean and unit variance which is uncorrelated for different pairs (ij) of beads and different time steps. The dissipation strength and the random noise strength together fix the temperature via the fluctuation–dissipation relation [21]

$$\sigma_{ij}^2 = 2\gamma_{ij}k_{\mathrm{B}}T. \tag{3}$$

Using these definitions, DPD corresponds to a description of the system of interest in the canonical NVT ensemble.

The non-bonded interaction between any two beads within the interaction range r_0 is soft-repulsive, and the force in the standard DPD model [23, 21, 22] is given by

$$\mathbf{F}_{ij}^{\mathrm{C}} = \begin{cases} a_{ij}(1 - r_{ij}/r_0)\hat{\mathbf{r}}_{ij}, & r < r_0, \\ 0, & r \geqslant r_0, \end{cases} \tag{4}$$

where a_{ij} is the interaction energy between beads i and j.

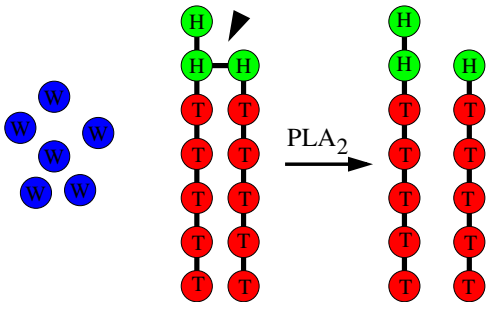

Figure 1. Definition of beads in the DPD simulations. Water (W) is represented by single beads. The $H_3(T_6)_2$ lipid model is composed of two linear chains of hydrophobic tail beads (T) connected by hydrophilic head beads (H). The cleavage site is indicated by an arrowhead and the product of cleavage after PLA_2 action is shown to the right: a lysolipid (left) and a fatty acid (right).

Table 1. Interaction energies for the repulsive interactions between the different beads in units of k_BT as used in the simulations. The value in parenthesis refers to the bond to be cleaved. See the text for discussion of the parameters.

Bead pairs	a_{ij}	l_0	k_2	k_3
WW	25	—	—	—
HH	25	0.5 (0.3)	128	—
TT	25	0.5	128	10
WH	25	—	—	—
WT	75	—	—	—
HT	50	0.5	128	10

Within a model lipid (see figure 1), the connectivity is implemented via a simple Hookean spring associated with a potential

$$U_2(\mathbf{r}_i, \mathbf{r}_{i+1}) = \tfrac{1}{2}k_2(|\mathbf{r}_{i,i+1}| - l_0)^2. \tag{5}$$

To add stiffness to the tail, a bending potential

$$U_3(\mathbf{r}_{i-1}, \mathbf{r}_i, \mathbf{r}_{i+1}) = k_3[1 - \cos(\phi - \phi_0)] \tag{6}$$

is imposed, where the bond angle ϕ is defined via the scalar product $\cos\phi = \hat{\mathbf{r}}_{i-1,i} \cdot \hat{\mathbf{r}}_{i,i+1}$. We have chosen the preferred bond angle to be $\phi_0 = 0$ (no bending of the tails is energetically advantageous).

In the following, we set the interaction cut-off r_0, the bead mass m (all beads are taken to have the same mass), and the thermostat temperature k_BT to unity and we use these parameters as basic units. We further fix the bead density to $\varrho = 3/r_0^3$ and choose the dissipation and noise parameters for all beads to be $\sigma_{ij} = \sigma = 3$ and (via equation (3)) $\gamma_{ij} = \gamma = 9/2$. The latter definition differs slightly from the parameters used in [24] where the interactions σ_{ij} were chosen to be different for different bead species (with the values γ_{ij} modified accordingly to ensure the same thermostat temperature). Regardless of this difference, the equilibrium properties of the system should not be affected by the choice of the DPD thermostat parameter values.

To implement the actual simulations, we used the model lipid $H_3(T_6)_2$, which consists of two linear chains of hydrophobic tail beads (T), linked asymmetrically to three hydrophilic head beads (H) (see figure 1). Water beads (W) are modelled as single beads. We have chosen the interaction parameters a_{ij}, l_0, k_2, k_3 according to table 1. Using the same lipid model with slightly different parameters, it was shown in [24] that the bending rigidity κ and the area compression modulus K_A are somewhat overestimated. We therefore modified the interaction parameters to obtain better agreement of κ and K_A with experimental values (see below for details). We also found a better agreement of the lateral pressure profile with results from

molecular dynamics simulations [25–27]. To integrate the discretized equations of motion, we employed a variant of the velocity Verlet algorithm with $\Delta t = 0.02$ (see [28] for details on various DPD integrators). We would like to point out that the integration time step Δt has to be carefully chosen, i.e. not too large, in order to avoid subtle unphysical artifacts (see [28, 29] for a discussion on artifacts in DPD simulations).

To relate the data and parameters to SI units, we choose the length scale as $r_0 \approx 0.65$ nm (which yields a bilayer thickness $\ell \approx 4$ nm similar to DMPC membranes, cf figure 3). We furthermore fix the mass m to obtain the density of water: $m\varrho$ has to match 10^3 kg m^{-3}, i.e. $m \approx 3.3 \times 10^{-25}$ kg. Extracting timescales requires a somewhat more sophisticated approach: from the DPD parameters, we are given a basic length scale, r_0, and timescale $\tau_0 = \sqrt{m r_0^2/(k_B T)}$, where we have already chosen the corresponding SI length scale. To fix the timescale, we measured the diffusion coefficient of lipids in an equilibrated membrane in DPD units ($0.021\,83\, r_0^2/(\nu\tau_0) \approx 1.6 \times 10^9$ nm$^{-2}/(\nu$ s)) and re-scaled the time via the free factor ν to match the experimental value of $\approx 4\ \mu$m^2 s^{-1} [30]. This was achieved for $\nu \approx 405$, i.e. $\Delta t = 0.02\ \tau_0$ corresponds roughly to 46 ps real time. Since our simulations were typically performed over 10^5 iterations, we cover a real time of 4.6 μs. The total CPU time for each simulation with 10^5 iterations was 7 h.

To derive the thermo-mechanical properties of the membranes from the DPD simulations, we used the following procedure. The area compression modulus K_A was calculated from the fluctuations of the area [31, 32], i.e.

$$K_A = \frac{k_B T \langle A \rangle}{\langle \delta A^2 \rangle}, \tag{7}$$

where $\langle A \rangle$ is the average projected area in the bilayer plane and $\langle \delta A^2 \rangle$ is the average of the squared fluctuations around the mean. The bending rigidity κ was calculated using linear-response theory (see [33, 34]): we applied a very weak sinusoidal force field given by $F(x) = F_0 \sin(qx)$ in the x-direction to the beads of the lipids. In response to the force field, the bilayer assumes on average a slightly sinusoidal form with an amplitude A_0. The bending rigidity can then be found for a tensionless bilayer from the equation

$$\kappa = \frac{f_0}{A_0 q^4}, \tag{8}$$

where f_0 is the force per area and $q = 2\pi/L_x$. This method yields the bending rigidity quickly and with small errors.

The lateral pressure profile across the membrane was calculated using the approach outlined in [35, 24]. In brief, the simulation box is partitioned into thin slabs parallel to the bilayer plane to be able to resolve the pressure tensor along the normal of the bilayer (z-direction). A weight function smooths out the configurational contribution to the pressure tensor arising from the conservative forces between two beads in an even fashion related to the slabs in between the aforementioned beads (taking into account the periodic boundary conditions).

3. Equilibrium properties of membranes in the absence of PLA_2 action

We first checked that a pre-assembled lipid bilayer remained stable when integrating the equations of motion. To this end we arranged the model lipids in a crystalline-like configuration along the mid-plane of the simulation box and distributed the water beads randomly above and below the interface. During the simulation we employed periodic boundary conditions. We also used a recently discussed barostat [32] to keep the bilayer at zero tension. The bilayer

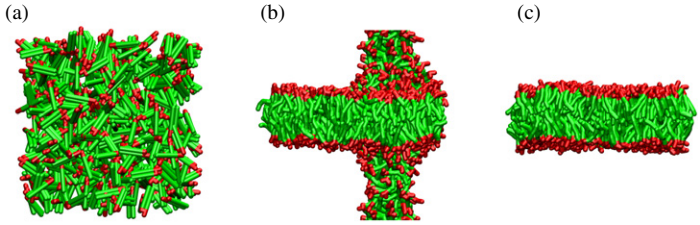

Figure 2. Snapshots of a self-assembling tensionless membrane from a random initial configuration (a). For intermediate times (b), the periodic boundary conditions support the formation of a stalk that collapses as the equilibrium configuration (c) is reached. Hydrophilic beads are shown in green and hydrophobic beads in red. The water beads are not shown.

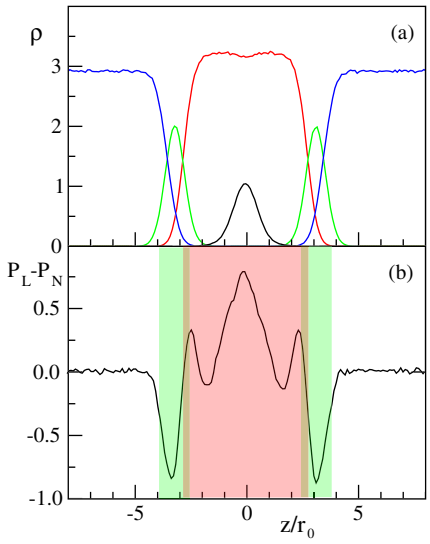

Figure 3. (a) Bead density profile for an equilibrated membrane. Water beads (blue) do not penetrate the membrane. Head beads (green) mark the hydrophilic interface, while the inner part of the bilayer is populated by the hydrophobic tail beads (red). The terminal tail beads (black) are concentrated in the mid-plane of the bilayer, showing the proper orientation of the lipids and the anticipated lack of interdigitation. (b) The lateral pressure profile $P_{\mathrm{L}} - P_{\mathrm{N}}$ shows pronounced peaks which agree qualitatively with Molecular Dynamics simulations. Colour shadings highlight the head group region (green) and the hydrophobic core (red), respectively.

was stable and had zero tension when using $N = 588$ model lipids in a cubic water box with an average edge length in the plane of the bilayer given by $L_x = L_y = 20$. The total number density was set to $\varrho \approx 3$ which gave a total of 240 00 beads. We next confirmed that a random dispersion of $N = 588$ model lipids in a water box of length $L_x = L_y = 20$ resulted in a stable, tensionless bilayer (see snapshots in figure 2). The final number density distribution, $\rho(z)$, of the different types of beads along the normal z-direction was the same for both initial conditions (figure 3(a)): water (W) was present above and below the formed interface, having little overlap with the hydrophilic head beads (H) and no overlap with the hydrophobic tail beads (T). The hydrophobic region did not contain hydrophilic head beads and the final tail beads all localized in the mid-plane of the bilayer, showing that the model lipids attained the anticipated ordering.

From the lateral pressure, $P_{\mathrm{L}}(z)$, and the normal pressure, $P_{\mathrm{N}}(z)$, we calculated the lateral pressure profile $P_{\mathrm{L}}(z) - P_{\mathrm{N}}(z)$ of the bilayer from successive uncorrelated snapshots every 200th integration step in the steady state. As can be seen from figure 3(b), the lateral pressure profile has a distinct shape featuring a large tensile pressure in the hydrophobic–hydrophilic interface and an expansive pressure in the hydrophobic core of the bilayer. The integral over the (negative) lateral pressure profile determines the membrane tension, which was near to zero as anticipated from the used barostat which enforced a tensionless state.

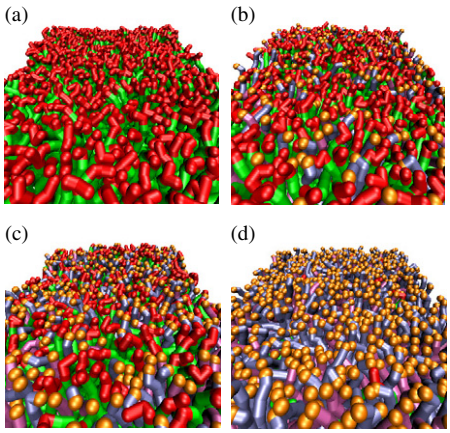

Figure 4. Representative snapshots of the upper surface of the equilibrated membrane when (a) $f_c = 0\%$, (b) $f_c = 25\%$, (c) $f_c = 50\%$, and (d) $f_c = 100\%$ of the lipids in the upper leaflet have been cleaved by PLA_2. Uncleaved lipids are shown in red/green (T/H), lysolipids in blue/gold, and fatty acids in purple/gold. An increased surface roughness can be observed.

The bending rigidity $\kappa = (16.3 \pm 0.7)k_BT$ fits well with the experimental value of a DMPC bilayer which has been measured by different techniques to lie in the range from 13 k_BT [36] to 30 k_BT [37]. From equation (7) the area compression modulus is found to be 0.312 ± 0.028 N m^{-1}, which deviates somewhat from the experimental value $K_A = 0.145$ N m^{-1} for DMPC [36]. Interestingly, from the membrane thickness $\ell \approx 4$ nm (cf figure 3) and the bending rigidity κ one obtains via the elasticity formula derived in [38]

$$K_A = \frac{48\kappa}{\ell^2} \tag{9}$$

an area compression modulus $K_A \approx 0.21$ N m^{-1} which agrees better with the experimental value. While this could indicate that the overestimation of K_A via equation (7) may be due to additional entropic contributions like undulation modes (see, e.g., [39] for a discussion of these effects), it is more likely that the used simulation parameters are not yet optimal. We would like to note, however, that we find $\kappa \approx 71\ k_BT$ and $K_A \approx 0.58$ N m^{-1} when using the parameters from [24] for the $H_3(T_6)_2$ model.

4. Equilibrium properties of membranes after PLA_2 action

To explore the influences of PLA_2 on the unperturbed and tensionless membrane, we took the following approach: we let a pre-formed, intact membrane equilibrate to a tensionless state using the barostat. After equilibration of the membrane we instantly cleaved a random fraction f_c of the lipids in the upper leaflet and then monitored the equilibration process with the barostat still on. We have chosen not to model PLA_2 explicitly as its diffusion and rate of cleavage may only be captured within very extensive and time-consuming simulations due to the somewhat bigger length and timescales. Our simulations thus describe the effect of a massive wave of PLA_2 molecules that attack the membrane at a given time, or a small patch recently attacked by several PLA_2 molecules.

Using the approach outlined above, we found that with increasing portions of cleaved lipids f_c, the membrane integrity is not affected during the simulation time but the surface showed an increasing roughness (see figure 4). This roughness may be gauged by inspecting the mechanical properties of the membrane: (i) the bending rigidity κ, which measures how prone a membrane is to undulations on the various length scales, and (ii) the area compression modulus K_A, that measures the resistance of the membrane to changes in its surface area. While for $f_c = 0$ both parameters are well within the range that is expected for fluid membranes [40],

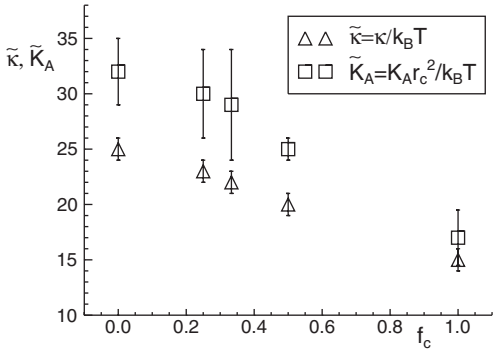

Figure 5. Bending rigidity κ and area compression modulus K_A as a function of the cleaved fraction f_c of lipids in the upper leaflet. While the unaffected state agrees well with experimental values of DMPC membranes [40], a dramatic decrease of these mechanical constants is observed as more and more lipids have been cleaved by PLA_2.

a strong decrease is observed as more and more lipids are cleaved (figure 5). As a consequence, the membrane is softened and becomes prone to rupture, although the presence of the hydrolysis products does not directly induce a collapse of the bilayer. It should be noted that the change in the projected surface area, A, needed to maintain the tensionless state was found to be small, e.g. from $f_c = 1/4$ to 1 a change in A of less than 5% was observed.

Concomitantly to the change of elastic constants an increase in the in-plane diffusion coefficient D within the membrane was observed (see table 2), especially for the partly digested leaflet. The action of PLA_2 leads approximately to a twofold higher mobility, indicating that the cleavage may also facilitate the diffusion of all peripheral membrane proteins. Since the mobility of lipids in the lower leaflet also increases slightly, one may also expect a somewhat higher diffusion coefficient for integral membrane proteins. Thus, membrane-bound processes like enzymatic reactions may be affected by PLA_2 via a change of the overall diffusive properties on the membrane.

Not only mechanical and diffusive properties of the membrane are altered, but the cleavage also leads to a secondary reorganization of the bilayer. While the cleavage products initially were distributed randomly in the upper leaflet, a fraction of these products undergoes a flip to the lower leaflet. In particular, the fatty acid residues of the cleaved lipids show a strong tendency of flip to the lower, intact leaflet whereas uncleaved lipids and lysolipids maintain their positions (see figure 6). Cleaving only low amounts does apparently not immediately enhance the flipping rate, yet for increasing levels of cleavage products a sigmoidal increase in the number of flipping events n_{flip} is observed. The action of PLA_2 may thus lead to an increased exchange of lipid material between the two leaflets, which enhances the dynamical features of biomembranes.

5. Discussion and conclusion

We have in the present paper investigated the action of a prototype of a molecular nano-machine, PLA_2, that is very common in biological systems. PLA_2 is a water-soluble enzyme that is only active at organized substrates of phospholipids, such as liposomes or the lipid-bilayer component of biological membranes. The enzymology of PLA_2 is complicated [41] and the details of the mechanism of action still remain to be resolved. From a physics perspective, the action of PLA_2 on lipid bilayers is challenging since it refers to an intrinsically non-equilibrium system where an initially one-component system is gradually turned into a ternary

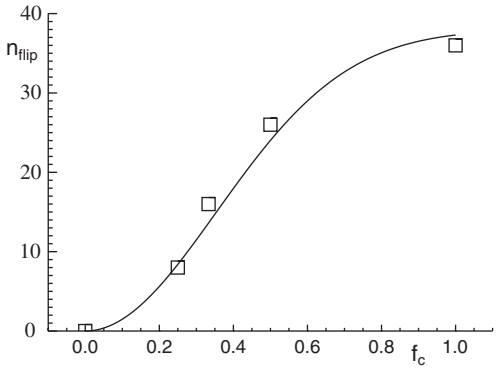

Figure 6. The number, n_{flip}, of flipping fatty acid residues increases sigmoidally with increasing PLA_2 action, i.e. with increased levels f_c of cleavage products. The full line is an empiric guide to the eye.

Table 2. Relative diffusion coefficients D/D_0, where $D_0 = 0.021\,83$ is the diffusion coefficient of an uncleaved lipid in an unperturbed membrane ($f_c = 0$). A clear increase of the mobility in the partly digested upper leaflet is seen as more and more lipids are cleaved. Values in brackets denote the diffusion of uncleaved lipids in the lower leaflet.

f_c	D/D_0 (phospholipid)	D/D_0 (fatty acid)	D/D_0 (lysolipid)
1/4	—	1.78	1.51
1/3	1.21 (1.29)	1.43	1.69
1/2	1.50 (1.35)	2.55	2.25
1/1	—	2.33	2.42

mixture. Earlier very simple modelling and simulation based on Monte Carlo simulation on lattice-gas models [16, 17] have tried to account for the non-equilibrium nature of the reaction and among other things been able to rationalize and reproduce the characteristic lag–burst behaviour observed under certain experimental reaction conditions [11]. Other theoretical work has proposed and clarified, in good accordance with available experimental data, that the enzyme becomes activated by single-lipid molecule protrusion modes that become enhanced by the softness of the bilayer [19, 20]. When a lipid molecule performs an excursion out of the bilayer, it is assumed to be more prone to hydrolysis.

None of the earlier theoretical work has taken the full self-assembly properties of the lipid bilayer in water into account when studying the action of PLA_2. By using the powerful simulation methods of DPD, the present paper represents an attempt to analyse the action of PLA_2 by simulating the effects of the presence of varying amounts of the hydrolysis products, lysolipid and free fatty acid, in the bilayer without attempting to model the enzyme itself. Neither does the approach take into account the non-equilibrium aspects of formation of the ternary mixture out of the pure phospholipid bilayer. However, our approach leads to new theoretical predictions regarding the effect of the hydrolysis products on the thermo-mechanical and diffusional properties of the bilayer. The results show, in good accordance with experimental findings, that the bilayer is considerably softened by the products, and the lateral diffusion is enhanced. Under the chosen conditions, the bilayer integrity is not compromised, which appears to be in accordance with experimental findings for certain unsaturated lipids [19] and in contact to experimental findings for certain saturated lipids [42]. In order to facilitate a closer comparison with experiments, a more complete model would have to be devised

which takes proper account of the direct effects of the lipase on the lipid bilayer, including the non-equilibrium conditions.

Acknowledgments

This work was supported by the BIOMS initiative in Heidelberg. The MEMPHYS-Center for Biomembrane Physics is supported by the Danish National Research Foundation. AFJ gratefully acknowledges support by an EMBO short term fellowship. MW was partly supported by BioNET-Danish Center for Biophysics, funded by the Villum Kann Rasmussen Foundation.

References

[1] Alberts B, Bray D, Lewis J, Raff M, Roberts K and Watson J D 1994 *Molecular Biology of the Cell* 3rd edn (New York: Garland Publishing)
[2] Elsner M, Hashimoto H and Nilsson T 2003 *Mol. Membr. Biol.* **20** 221
[3] Kirchhausen T 2000 *Nat. Rev. Mol. Cell Biol.* **20** 187
[4] Six D A and Dennis E A 2000 *Biochim. Biophys. Acta* **1488** 1
[5] Chakraborti S 2003 *Cell. Signal.* **15** 637
[6] Jupp O J, Vandenabeele P and MacEwan D J 2003 *Biochem. J.* **374** 453
[7] Laye J P and Gill J H 2003 *Drug Discov. Today* **8** 710
[8] Andresen T L, Jensen S S and Jørgensen K 2005 *Prog. Lipid Res.* **44** 68
[9] Hønger T, Jørgensen K, Stokes D, Biltonen R L and Mouritsen O G 1997 *Methods Enzymol.* **286** 168
[10] Nielsen L K, Risbo J, Callisen T H and Bjørnholm T 1999 *Biochim. Biophys. Acta* **1420** 266
[11] Hønger T, Biltonen R L, Jørgensen K and Mouritsen O G 1996 *Biochemistry* **35** 9003
[12] Apitz-Castro R, Jain M K and De Haas G H 1982 *Biochim. Biophys. Acta* **688** 349
[13] Grandbois M, Clausen-Schaumann H and Gaub H 1998 *Biophys. J.* **74** 2398
[14] Nielsen L K, Risbo J, Callisen T H and Bjørnholm T 1999 *Biochim. Biophys. Acta* **1420** 266
[15] Leidy C, Mouritsen O G, Jørgensen K and Peters G H 2004 *Biophys. J.* **87** 408
[16] Høyrup P, Callisen T H, Jensen M Ø, Halperin A and Mouritsen O G 2004 *Phys. Chem. Chem. Phys.* **6** 1608
[17] Høyrup P, Jørensen K and Mouritsen O G 2002 *Europhys. Lett.* **57** 464
[18] Raudino A 1998 *Eur. Phys. J.* **2** 197
[19] Høyrup P, Jørgensen K and Mouritsen O G 2002 *Comput. Phys. Commun.* **147** 313
[20] Halperin A and Mouritsen O G 2005 *Eur. Biophys. J. Biopys. Lett.* at press
[21] Español P and Warren P 1995 *Europhys. Lett.* **30** 191
[22] Groot R D and Warren P B 1997 *J. Chem. Phys.* **107** 4423
[23] Hoogerbrugge P J and Koelman J M V A 1992 *Europhys. Lett.* **19** 155
[24] Shillcock J C and Lipowsky R 2002 *J. Chem. Phys.* **117** 5048
[25] Lindahl E and Edholm O 2000 *J. Chem. Phys.* **113** 3882
[26] Gullingsrud J and Schulten K 2004 *Biophys. J.* **86** 3496
[27] Sonne J, Hansen F Y and Peters G H 2005 *J. Chem. Phys.* **122** 124903
[28] Nikunen P, Karttunen M and Vattulainen I 2003 *Comput. Phys. Commun.* **153** 407
[29] Jakobsen A F, Mouritsen O G and Besold G 2005 *J. Chem. Phys.* at press
[30] Korlach J, Schwille P, Webb W W and Feigenson G W 1999 *Proc. Natl Acad. Sci. USA* **96** 8461
[31] Feller S E and Pastor R W 1999 *J. Chem. Phys.* **111** 1281
[32] Jakobsen A F 2005 *J. Chem. Phys.* **122** 124901
[33] Lomholt M A, Hansen P L and Miao L 2005 *Eur. Phys. J.* **16** 439
[34] Lomholt M A, private communication
[35] Goetz R and Lipowsky R 1998 *J. Chem. Phys.* **108** 7397
[36] Evans E and Rawicz W 1990 *Phys. Rev. Lett.* **64** 2094
[37] Lee C H, Lin W C and Wang J 2001 *Phys. Rev.* E **64** 020901
[38] Goetz R, Gompper G and Lipowsky R 1999 *Phys. Rev. Lett.* **82** 221
[39] Feller S E and Pastor R W 1999 *J. Chem. Phys.* **111** 1281
[40] Mouritsen O G 2005 *Life-As a Matter of Fat. The Emerging Science of Lipidomics* (Berlin: Springer)
[41] Berg O G, Gelb M H, Tsai M D and Jainet M K 2001 *Chem. Rev.* **101** 2613
[42] Callisen T H and Talmon Y 1998 *Biochemistry* **37** 10987